

# Omni-ID: Holistic Identity Representation Designed for Generative Tasks

Guocheng Qian Kuan-Chieh Wang Or Patashnik Negin Heravi  
 Daniil Ostashev Sergey Tulyakov Daniel Cohen-Or Kfir Aberman  
 Snap Research

<https://snap-research.github.io/Omni-ID>

## Abstract

We introduce *Omni-ID*, a novel facial representation designed specifically for generative tasks. *Omni-ID* encodes holistic information about an individual’s appearance across diverse expressions and poses within a fixed-size representation, where each entry represents certain global or local identity features. Our approach uses a few-to-many identity reconstruction training paradigm, where a limited set of input images is used to reconstruct multiple target images of the same individual in various poses and expressions. A multi-decoder framework is further employed to leverage the complementary strengths of diverse decoders during training. Unlike conventional representations, such as CLIP and ArcFace, which are typically learned through discriminative or contrastive objectives, *Omni-ID* is optimized with a generative objective, resulting in a more comprehensive and nuanced identity capture for generative tasks. Trained on our MFHQ dataset – a multi-view facial image collection, *Omni-ID* demonstrates substantial improvements over conventional representations across various generative tasks.

## 1. Introduction

Generating images that faithfully represent an individual’s identity requires a face encoding capable of depicting nuanced details across diverse poses and facial expressions. However, a significant limitation of existing facial representations [7, 21, 32, 40] is their reliance on single-image encodings, which fundamentally lack holistic information about one’s appearance. For example, an image of someone in a frontal pose with a neutral expression reveals little about how they look when smiling, frowning, or viewed from their profile.

Furthermore, existing face representation methods, typically derived from networks optimized for discriminative tasks such as ArcFace [7] or text-aligned image encoders

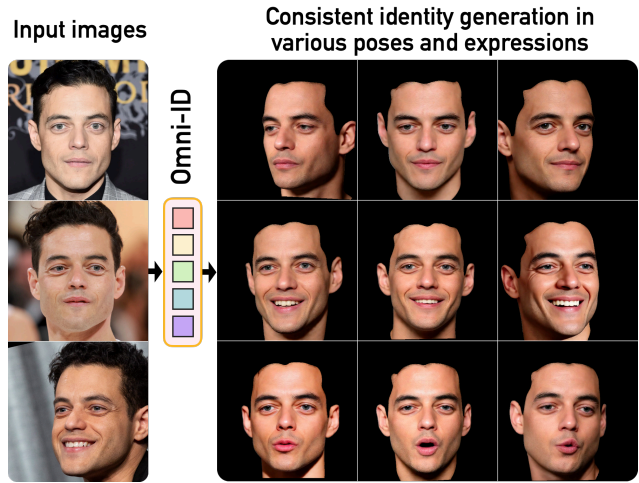


Figure 1. *Omni-ID* is a facial representation that consolidates information from a varied number of images of an individual into a fixed-size, structured encoding. Each element of this encoding captures specific global or local identity features, enabling high-fidelity generation in new poses, expressions, and capturing identity-consistent variations.

like CLIP [21], are not well suited for generative applications. While these models effectively distinguish between individuals or extract semantic features, they are constrained by a discriminative bottleneck that omits fine-grained identity details. Consequently, they struggle to capture the subtle nuances that define a person’s unique identity, especially across different poses and expressions, as demonstrated in Fig. 2.

In this work, we introduce *Omni-ID*, a facial identity representation designed for generative tasks. *Omni-ID* encodes a varied number of images of an individual into a compact, fixed-size representation, capturing the individual in diverse expressions and poses as shown in Fig. 1. This enriched encoding can be used in a wide range of generative tasks, maximizing the faithful preservation of the individual’s subtle details across various contexts.

At the core of the approach lies our *Omni-ID* encoder

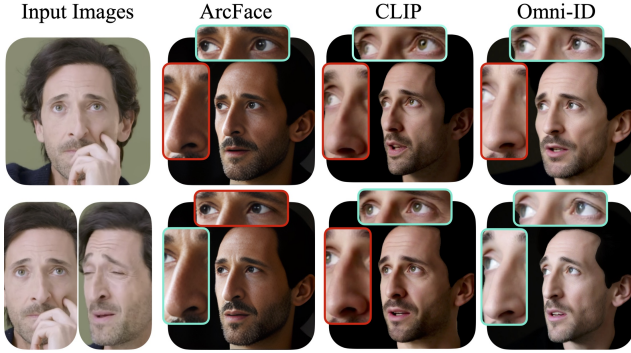


Figure 2. **Face generation comparison of different facial representations** with single input (top row) and two inputs (bottom row). We evaluate different facial representations by training an IP-adapter [37] on FLUX [3] with each representation. It can be seen that single-instance representations such as ArcFace and CLIP struggle to combine unique features appear in each observation (e.g., eye color and nose shape), whereas our Omni-ID, designed with a *few-to-many* generative objective, improves identity representation with each additional view, unifying unique attribute from multiple views into a single representation.

trained within a generative framework (illustrated in Fig. 4) that leverages two key ideas. First, the framework uses a *few-to-many identity reconstruction* training paradigm that not only reconstructs the input images but also a diverse range of other images of the same identity in various contexts, poses, and expressions. This strategy encourages the representation to capture essential identity features observed across different conditions while mitigating overfitting to specific attributes of any single input image. Second, our framework employs a *multi-decoder* training objective that combines the unique strengths of various decoders, such as improved fidelity or reduced identity leakage, while mitigating the limitations of any single decoder. This enables leveraging the detailed facial information present in the input images to the greatest feasible degree and results in a more robust encoding that effectively generalizes across various generative applications.

Our Omni-ID encoder is transformer-based and employs a fixed-size set of learnable queries to produce a consistent, fixed-size representation of an individual’s identity. This design ensures that regardless of the number of input images provided, the encoder yields a structured encoding by blending the input images via keys and values throughout attention layers. The fixed-size representation is essential for downstream applications, as it establishes a ‘structured’ encoding where each feature within the representation can correspond to specific identity attributes, such as different facial regions as visualized in Fig. 10. Structured representations allow downstream tasks to focus on learning from the distilled identity features without being distracted by the

noise and variability present in individual input images.

To validate Omni-ID’s effectiveness, we conduct extensive experiments comparing our method against state-of-the-art baselines, including ArcFace [7] and CLIP [21] representations. Notably, with our representation the generation quality scales with the number of input images, enabling it to capture a more comprehensive view of the individual, as shown in Fig. 2. In addition, we demonstrate Omni-ID’s superiority in two widely used face generative tasks: controllable face synthesis and personalized text-to-image generation. Extensive experiments show that Omni-ID significantly improves identity preservation across a range of poses, expressions and contexts, achieving higher fidelity in generating photorealistic images.

## 2. Related work

**Face representation** provides a foundation for 3D face reconstruction, accurately distinguishing identities and synthesizing realistic face images. Parametric 3D Morphable Models [4, 5, 18] have been historically used to represent face shape geometry through identity and expression blendshapes combined with pose. However, these representations are coarse and lack the appearance details needed for photo-realistic generation. In recognition tasks, approaches like CosFace [32] and ArcFace [7] have improved identity discrimination by utilizing a margin loss, which enhances intra-class compactness and inter-class separability, and have also been widely applied in generation tasks. More recently, FaRL [40] creates a more descriptive facial token representations by fine-tuning the pretrained visual model, CLIP [21] on large-scale face-text paired datasets. In contrast to these discriminative or contrastive facial identity representations, our Omni-ID is optimized with a generative objective, resulting in a more nuanced identity representation well suited for generative tasks.

**Face synthesis** has evolved significantly, starting with StyleGAN [17], which set new standards for high-quality, realistic face generation through a well-structured latent space. However, StyleGAN offered limited control over individual facial features. To address this, researchers introduced methods to invert real images into StyleGAN’s latent space [1, 2, 13, 22, 30], enabling attribute manipulation by altering latent codes. Given recent advances in generative models, diffusion [8, 14, 15, 29] and flow-based [23] generative models offer even higher quality generations than GAN-based approaches. In Sec. 4.2 we study controllable face generation and show improved identity fidelity when using our proposed face representation.

**Personalized text-to-image generation** embeds specific visual elements or concepts that are unique to individual users or classes of images to text-to-image models [15, 24]. Early works focused on introducing new tokens or fine-tuning model weights to represent personalized content



Figure 3. **Gallery of Omni-ID in personalized T2I generation.** Omni-ID enables high identity preservation. Results achieved by injecting Omni-ID representation through IP-Adapter [37] into the frozen FLUX dev model [3] without LoRA [16].

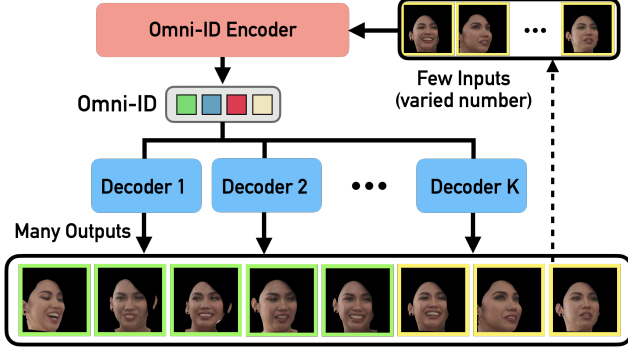


Figure 4. Omni-ID employs a *multi-decoder few-to-many identity reconstruction* training strategy, incorporating three key design features: (1) An encoder that learns a unified, fixed-size identity representation from a varied number of inputs; (2) A few-to-many identity reconstruction task, designed to generate multiple faces of an individual in various poses and expressions from a limited set of samples of the same individual; (3) A multi-decoder training strategy that combines the unique strengths of various decoders while mitigating the limitations of any single decoder.

while maintaining the prior of the model [9, 16, 26, 31]. Since then, feedforward methods were introduced to reduce the computational cost from per-subject optimization [27, 37]. These techniques typically utilized encoders [10] or adapters [28, 33] that process images into representations then directly inject into text-to-image models during inference. A major focus of research has been placed on personalizing text-to-image models for human faces. IP-Adapter [37] proposed to inject faces through decoupled attention layers. Follow-ups improve identity preservation and controls by ControlNet [34, 39], text embedding merging [19], and face identity loss [11, 12]. However, existing personalization approaches rely on facial representations derived from single-instance encodings, extracted from networks trained with discriminative objectives. Orthogonal to these efforts, our work focuses on identity representation compatible with the different approaches. We show that Omni-ID representation improves personalized generation when compared to other face representation using the same personalization approach.

### 3. Method

Let  $\mathcal{X} = \{x_1, x_2, \dots, x_M\}$  represent a set of  $M$  input images of an individual where each image  $x_i \in \mathbb{R}^{H \times W \times 3}$  depicts the individual’s face under varying poses, expressions, and lighting conditions. Our goal is to create a holistic facial identity representation,

$$\ell = E(\mathcal{X}), \quad (1)$$

that captures an individual’s appearance and its nuanced variations across different contexts, poses, and expressions.

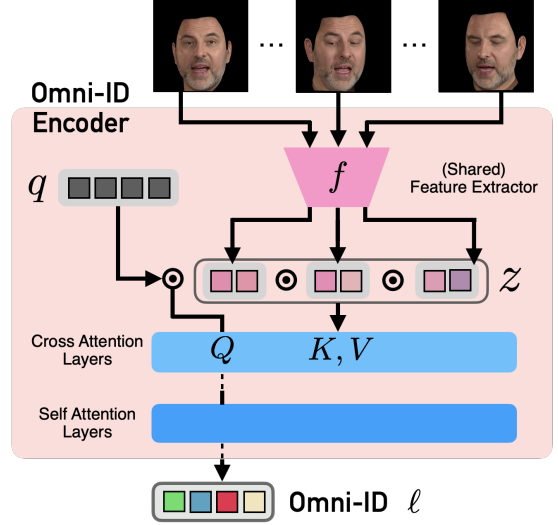


Figure 5. **Omni-ID Encoder** receives a set of images of an individual, projects them into keys and values, which are then fed into cross-attention layers. These layers attend to **learnable queries** that are semantic-aware, allowing the encoder to capture shared identity features across images. Self-attention layers refine these interactions further, producing a holistic representation  $\ell$ .

To this end, we introduce a new face representation named Omni-ID, featuring an Omni-ID Encoder and a novel *few-to-many identity reconstruction* training with a *multi-decoder* objective. Designed for generative tasks, this representation aims to enable high-fidelity face generation in diverse poses and expressions, supporting a wide array of generative applications.

In the following, Sec. 3.1 describes our the Omni-ID encoder architecture. Sec. 3.2 details the few-to-many identity reconstruction task used during training. Sec. 3.3 discusses the multi-decoder objective, which has two complementary decoding objectives, each applied within the few-to-many identity reconstruction framework. Lastly, Sec. 3.4 introduces the dataset we curated to maximize the potential of the proposed training strategy.

#### 3.1. Omni-ID Encoder

Our proposed Omni-ID Encoder  $E$  encodes an image set  $\mathcal{X}$ , with any number of images, into a holistic representation for the identity  $\ell = E(\mathcal{X}) \in \mathbb{R}^{L \times C}$ .  $L$  represents the token length and  $C$  denotes the number of dimensions. In order to support encoding an image set, the key design decisions revolve around how to combine individual image features,  $\ell = f(x_i) \in \mathbb{R}^{L_x \times C}$ , where  $L_x$  is the token length for the image features. For this, we use a transformer architecture with a learnable token  $q \in \mathbb{R}^{L \times C}$ . The individual image features are first concatenated in the token-axis to form the image set feature,  $z = [\ell_0; \ell_1; \dots; \ell_M] \in \mathbb{R}^{(M \cdot L_x) \times C}$ , and then integrated in the encoder through cross-attention

layers as keys and values. Our full transformer architecture consists of multiple cross-attention layers (all with KV-injection from  $z$ ) followed by multiple self-attention layers. See Fig. 5 for an overview of our architecture.

### 3.2. Few-to-Many Identity Reconstruction

During training, given the full set of images of an individual,  $\mathcal{X} = x_1, x_2, \dots, x_N$ , we randomly select a small input subset  $\mathcal{X}^s$ , and another larger set  $\mathcal{X}^r$  as reconstruction targets, where  $|\mathcal{X}^r| > |\mathcal{X}^s|$ . The model is tasked with utilizing the input subset  $\mathcal{X}^s$  for generating the target subset  $\mathcal{X}^r$ .

Given the encoder feature  $\ell$ , each of the decoders  $D$  is tasked to conditionally reconstruct all the target images:

$$\hat{x}_i^r = D(\ell, \tilde{x}_i^r), \quad \forall x_i^r \in \mathcal{X}^r, \quad (2)$$

$$\tilde{x}_i^r = \text{Corruption\_Process}(x_i^r), \quad (3)$$

where  $\tilde{x}_i^r$  is the corrupted target image. Intuitively, a corruption process destroys information from the target image, and prevents the decoder from utilizing the target image to achieve autoencoding. This forces the decoder to rely on the encoder feature  $\ell$  to infer identity information, thereby encouraging the encoder to learn a robust identity representation. Meanwhile, the corrupted target image still retains cues about other conditions, such as lighting, pose, and subtle hints of expression, providing essential context that, when combined with representation from the encoder, enables accurate reconstruction. To leverage the strengths of different corruption types, we employ distinct objectives, which we detail below.

### 3.3. Multi-Decoder Objectives

Our multi-decoder objective optimizes a single encoder by  $K$  distinct decoders. In our design, we utilize two (i.e.,  $K=2$ ) complementary decoding objectives: a conditional masked reconstruction objective referred to as the Masked Transformer Decoder (MTD) and a conditional Flow-Matching objective. The MTD objective is suitable for learning a representation with wide coverage, but on its own suffers from neglecting fine-grained details. The Flow-Matching objective excels at picking up fine-grained details by training at various noise levels, but on its own is less effective for representation learning (shown in Sec. 4.4).

**Decoder 1: Masked Transformer Decoder** Our first decoding objective is a variant of conditional masked autoencoding we call *Masked Transformer Decoder* (MTD), where the decoder receives as inputs the Omni-ID representation  $\ell$ , and a heavily masked version of targets to reconstruct (i.e. 95% of tokens masked). By applying a very high masking ratio, MTD ensures subject’s anonymity and that the identity information is solely derived from  $\ell$ . The minimal visible/unmasked pixels provide essential contexts

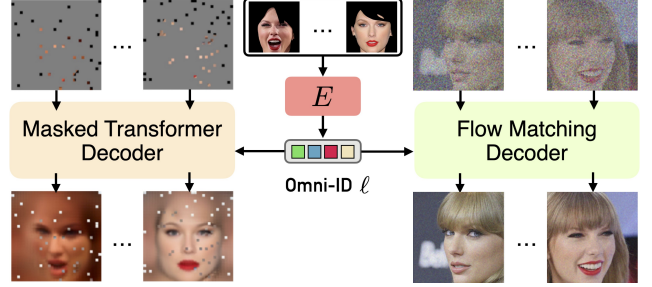


Figure 6. **Multi-decoder training.** (left) Masked Transformer Decoder (MTD) is designed to reconstruct unseen facial pixels from the Omni-ID representation and a minimal subset of visible pixels which do not leak identity. (right) Flow Matching Decoder enhances the encoder by a higher-quality reconstruction task.

such as pose and lighting. The Omni-ID Encoder and the Masked Decoder  $D$  are trained end-to-end using a reconstruction loss as follows:

$$\mathcal{L}_1 = \frac{1}{|\mathcal{X}^r|} \sum_{x^r \sim \mathcal{X}^r} \left| (D(\ell, \tilde{x}^r) - x^r) \odot M^r \right|_1, \quad (4)$$

$$\ell = E(\mathcal{X}^s), \quad \tilde{x}^r = x^r \odot M, \quad (5)$$

where  $M$  is the randomly sampled mask to corrupt the target image  $x^r$  and  $M^r$  is the face segmentation mask to remove background. Refer to Fig. 6 (left) for a practical example of how inputs and masked prediction appear during MTD training. The decoder uses the same architecture as the Omni-ID encoder, but instead of a learned query, its query comes from the masked input target image  $\tilde{x}^r$ . The identity feature  $\ell$  is fed through the cross attention layers and serves as keys and values in the decoder.

**Decoder 2: Conditional Flow Matching** The MTD objective, being a variant of autoencoding, serves as an effective approach for learning a wide covering representation. However, it suffers from the pitfalls of an autoencoding objective, which tends to produce blurry outputs and omit fine-grained details. To capture more nuanced details, a decoder that is able to recover nuanced details is required. For this, we resort to diffusion decoders in conditional flow matching. These decoders are optimized to remove noise from a noisy target at various noise-levels encouraging our model to learn details at all noise-levels.

The Omni-ID Encoder and the diffusion decoder  $V$  are optimized jointly by flow matching objective:

$$\mathcal{L}_2 = \mathbb{E}_{x^r \sim \mathcal{X}^r, t, \epsilon} \left[ \left\| V(\tilde{x}_{t, \epsilon}^r, t, y, \ell) - (\epsilon - x^r) \right\|_2^2 \right], \quad (6)$$

$$\ell = E(\mathcal{X}^s), \quad \tilde{x}_{t, \epsilon}^r = (1 - t)x^r + t\epsilon, \quad (7)$$

where  $t \sim \mathcal{U}(0, 1)$  is the time step and  $\epsilon \sim \mathcal{N}(0, I)$  is a noise sample from the standard normal distribution and  $y$

is a fixed text prompt ("photo of a person."). Refer to Fig. 6 (right) for an example of how inputs and targets appear during Flow-Matching training. Decoder  $V$  is a combination of a pretrained flow model [3] and IP-Adapter [37]. Similarly to IP-Adapter, we project Omni-ID representation into keys and values and inject them via learnable decoupled attention layers into the pretrained flow decoder.

### 3.4. MFHQ Dataset

Omni-ID training requires a large-scale dataset with many identities, each with multiple face images. The closest existing datasets that meet this requirement are the ones used for face recognition, *e.g.* WebFace42M [42]. However, the quality of these datasets is insufficient to train generative face representations due to two major limitations. First, they are low-resolution (typically  $112 \times 112$ ), and the representations trained on the up-sampled versions of them tend to smooth out the fine-grained details [20]. Second, intra-identity variations in face recognition datasets are usually too high due to age and quality variations, making the generative representation trained on them unable to encode a consistent facial identity. Refer to Sec. 4.4 for examples.

We thus introduce a new large-scale dataset **MFHQ—multiple faces in high quality**. MFHQ consists of 134,077 identities with 8 images per ID collected from videos to ensure identity consistency. The face resolution is filtered to be larger than 448. MFHQ overclusters the video frames based on their estimated head poses, then samples 8 faces for each ID according to the face quality estimation [6]. This clustering-based sampling ensures pose differences. The video sources come from a combination of CelebV-HQ [41], VFHQ [36], TalkingHead-1KH [35], and CelebV-Text [38]. MFHQ collection is illustrated in *Appendix*.

## 4. Experiments

In this section, we validate the learned Omni-ID representation by evaluating its performance on two downstream generative tasks. In both tasks, we compare the Omni-ID representation to existing identity representations, demonstrating improved identity fidelity and adaptability.

The first task is *controllable face generation* (Sec. 4.2), where a downstream generator produces an image of an individual in unseen poses based on an identity representation and a target pose (*i.e.*, landmarks). This task tests the representation’s ability to capture nuanced changes with varying poses and expressions.

The second task is *personalized text-to-image generation* (Sec. 4.3). Here, the generator creates scene-level images that maintain both individual identity and the quality of the original text-to-image model. Our results on this task further validate that the Omni-ID representation outperforms existing alternatives and demonstrates its effectiveness in the popular application of personalized generation.

Table 1. **Quantitative comparisons to different representations** on controllable face generation. The backbone is the same for all methods: IP-Adapter + ControlNet. All baselines undergoes Flow-Matching pretraining to initialize IP-Adapters to converge for fair comparison. We show three results of using 1/3/5 inputs.

Method	ID Similarity $\uparrow$	Pose Error $\downarrow$
ArcFace	0.515 / 0.523 / 0.529	2.4 / 2.3 / 2.3
CLIP	0.648 / 0.670 / 0.680	2.3 / 2.3 / 2.2
ArcFace + CLIP	0.638 / 0.655 / 0.663	2.4 / 2.4 / 2.3
<b>Omni-ID (Ours)</b>	<b>0.708 / 0.728 / 0.737</b>	<b>2.1 / 2.0 / 2.0</b>

Lastly, we validate our design choices including each of the few-to-many identity reconstruction training paradigm, the decoding objectives, our proposed dataset, and their hyperparameters (Sec. 4.4).

### 4.1. Implementation Details

**Omni-ID encoder.** Our Omni-ID encoder uses CLIP-H [21] as the feature extractor and finetunes all layers. Omni-ID encoder uses a learnable query with  $L=256$ ,  $C=1280$  and 2 cross-attention blocks and 2 self-attention blocks, which is sufficient to learn a representation from image features.

**Omni-ID training.** Our MTD decoder is trained for 250K steps with a masking ratio of 95%. Our Flow-Matching Decoder is trained for 10K steps using FLUX dev [3] as the base model. Both stages are trained in MFHQ with 44 held out videos as testing and others as training. See *Appendix* for further training details.

**Baseline representations.** In the controllable face generation task, we compare our Omni-ID representation to other commonly used identity representations: pretrained CLIP features [21] and Arc-Face embedding [7]. We also compare to CLIP+ArcFace, following FaceIDPlus [37], where the ArcFace embeddings are projected into queries and CLIP features are used as keys and values to get the representation through the same attention mechanism as our Omni-ID. For CLIP representations, we use all 257 tokens for all baselines. For ArcFace, we project embedding  $\mathbb{R}^{1 \times 512}$  to 256 tokens  $\mathbb{R}^{256 \times 512}$  for better quality. For the personalized text-to-image generation task, we compare our Omni-ID representation to pretrained CLIP embedding. For both tasks, we ensure fair comparisons with the baselines by training the downstream models to convergence when using each of the representations (detailed in *Appendix*).

**Metrics.** We use ID similarity and pose error as the evaluation metrics in controllable face generation. ID similarity is measured using the standard cosine similarity between the ArcFace features extracted from the generation and ground truth. Pose error [25] is measured by the sum of absolute differences of yaw, pitch, roll in degrees.



Figure 7. **Qualitative comparisons in controllable face generation.** We train the same IP-Adapter+ControlNet for each representation. Omni-ID achieves superior identity preservation and captures nuanced changes with varying poses and expressions more faithfully.

## 4.2. Controllable Face Generation

Given a pretrained representation, we train a combination of ControlNet [39] and IP-Adapter with frozen FLUX for controllable face generation. The ControlNet receives as input landmark images of the target pose, where IP-Adapter injects frozen face representations. Methods are evaluated on the test set of MFHQ with 44 identities from the held-out videos. Compared to the ArcFace, CLIP, or their combined representations, the Omni-ID representation shows better performance in both identity preservation and pose accuracy (see Tab. 1). Beyond metrics, Fig. 7 highlights qualitative differences between representations using 5 inputs driven by template landmarks. While ArcFace encodes facial features effectively for recognition tasks, it is overly invariant to attributes like age and skin tone. CLIP preserves general visual features but struggles with adaptivity to new poses and expressions due to its instance-level encoding and lack of fine-tuning for facial details. Consequently, facial features such as beards (last row) are not accurately represented in CLIP, and sensitivity to pose and expression changes is noticeable. In contrast, Omni-ID achieves high-fidelity identity preservation, capturing detailed facial char-

acteristics across diverse pose and expressions.

## 4.3. Personalized T2I Generation

Given a pretrained representation, we train an IP-Adapter to inject into frozen FLUX-dev. Notice, this differs from the denoising decoder we used during representation learning in its data. Here, the input data is an image of the face, but the target image is a scene-level image and has a corresponding text caption. We train all baselines in the same internal licensed image dataset ( $\sim 1M$  single-view images), and evaluate them on 10 identities and 20 diverse prompts. ID similarity is employed as the metric. See Appendix for the quantitative results. As can be seen in Fig. 8, Omni-ID representation demonstrates superior performance in terms of identity preservation when applied to personalized text generation, outperforming CLIP in both single input image, as well as in the the multiple input images case. See Fig. 3 for more results of Omni-ID. See Appendix for more qualitative comparisons using different base models.






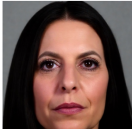
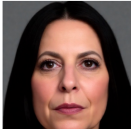
## 4.4. Ablations & Analyses

Tab. 2 summarizes experimental results where we used face generation qualities from our Flow-Matching decoder as



Figure 8. **Qualitative comparisons with different representations in personalized T2I generation.** We show results of the same IP-Adapter trained with different representations. Our Omni-ID achieves better ID preservation for both single and multiple input images. See more examples and how IP-Adapter+Omni-ID significantly outperforms other personalization methods [19, 34] in *Appendix*.

Table 2. **Validating MTD decoder and its design decisions.** This table summarizes the face generation quality from the Flow-Matching Decoder described in Sec. 3.3 with varied configurations in the MTD pre-training. For each configuration, we report results using 1 or 3 input image(s) (1-image / 3-image). ‘I-O’ denotes the number of input and output images used in training.

Ablation	Ours full	w/o MTD	Few-to-many			MTD mask ratio	
I-O, mask ratio	3-8, 0.95	—	3-1, 0.95	3-5, 0.95	8-8, 0.95	3-8, 0.99	3-8, 0.85
<b>ID Similarity</b> ↑	<b>0.683 / 0.733</b>	0.336 / 0.358	0.491 / 0.515	0.582 / 0.615	0.661 / 0.696	0.670 / 0.700	0.609 / 0.650
Inputs	Ours	w/o MTD	3-1	3-5	8-8	Mask 0.99	Mask 0.85
							

evaluation for different MTD pre-training configurations. We ablated the number of images used as inputs and targets during MTD pre-training, removing MTD completely and changing other hyperparameters. Tab. 3 summarizes experimental results of the downstream controllable face generation performance by using different checkpoints obtained by ablating the individual decoding objectives and using an alternative dataset [42] instead of our MFHQ.

**Few-to-many identity reconstruction.** Tabs. 2 and 3 demonstrates the few-to-many reconstruction task is better than the conventional alternative of single-image recon-

struction. In Tab. 2, we observed increasing performance as we increase the number of target images (compare 3-8 with 3-1 and 3-5). Note 3-8 outperforms 8-8 since the latter might reconstruct all inputs, whereas 3-8 is always optimized to also reconstruct unseen images with new poses and expressions. In Tab. 3, the performance significantly degrades when using single-image reconstruction for both decoding objectives (‘— Few-to-many pretraining’ row).

**MTD objective.** In Tab. 2, MTD pre-training results in better performance with generally a higher masking ratio. However, as the masking ratio reaches 99%, the perfor-



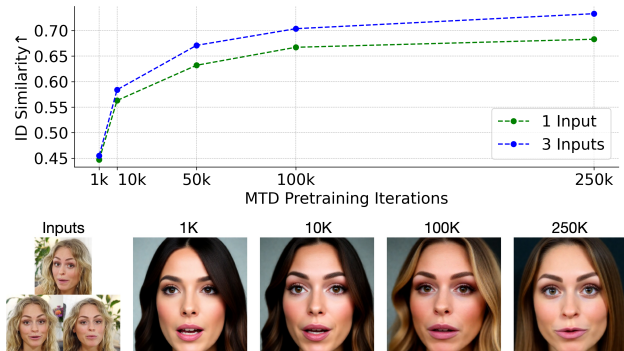


Figure 9. **More MTD pretraining consistently improves ID preservation.** That curve shows the quantitative results from 1 or 3 inputs with increasing *MTD pretraining* steps followed by the same Flow-Matching Decoder training steps for fair comparisons.

Table 3. **Ablate Flow-Matching Decoder training** evaluated in controllable face generation. Both Flow-Matching Decoder pretraining and MFHQ dataset enhances details. Few-to-many identity reconstruction training and MTD improve ID preservation.

Ablation	ID Similarity $\uparrow$	Pose Error $\downarrow$
Ours full	<b>0.708 / 0.728</b>	2.1 / 2.0
- MTD pretraining	0.468 / 0.473	2.8 / 3.1
- Flow-Matching Decoder pretraining	0.672 / 0.685	2.4 / 2.3
- Few-to-many pretraining	0.616 / 0.633	2.3 / 2.2
- Pretraining on MFHQ	0.678 / 0.693	2.2 / 2.1

Inputs	Ours	w/o MTD	w/o Flow-Matching Decoder	w/o Few-to-Many	w/o MFHQ

mance drops slightly. Intuitively, MTD benefits from a high masking ratio, but too high of a masking ratio also makes the reconstruction task ill-posed and noisy. In addition, Fig. 9 demonstrates MTD pretraining is beneficial for the Flow-Matching decoder training consistently at almost any number of steps and consistently improves encoding. Lastly, Tab. 3 shows that removing MTD pre-training harms the downstream controllable face generation.

**Flow-Matching objective.** As shown in Tab. 3, removing the Flow-Matching decoding objective leads to a lower identity similarity score and a noticeable loss of fine-grained details (e.g., less defined beards and smoother faces as shown in the figure). In the Flow-Matching decoder, due to the different noise-levels, it encourages the representation to encode the fine-grained details.

**Effectiveness of MFHQ.** Results in Tab. 3 validate the utility of our MFHQ dataset. When we replace our training data with the existing alternative, WebFace21M [20], we see a drop in the identity fidelity. This is due to the larger intra-class ID variation, which introduces noise in training.

**Attention visualization.** We visualize the attention maps of



Figure 10. **Visualization of attention maps** between individual learned query and the keys extracted from input images. Notably, different queries focus on distinct semantic and specific regions of the face. The learned queries also effectively adapt to variations in input facial features, such as open or closed mouths and eyes, as well as to occlusions like hands or missing features, such as ears.

our Omni-ID encoder in Fig. 10. Notably, the same learned token attends to different patches across various input images based on semantic context. For instance, the same query feature results in a different attention map depending on whether the eyes are open or closed, while queries focused on the mouth region ignore a hand occluding it. These results demonstrate that Omni-ID learns to consolidate visual information scattered across an unstructured set of input images into a structured representation, where each entry represents certain global or local identity features.

## 5. Conclusions

We introduced Omni-ID, a facial identity representation tailored for generative tasks, which captures an individual’s holistic appearance across various expressions and poses. Trained in a few-to-many identity reconstruction framework, the Omni-ID encoder encodes fine-grained facial features from diverse input images, demonstrating superior identity preservation. Unlike discriminative representations like ArcFace and CLIP, Omni-ID retains nuanced identity information critical for high-fidelity generative tasks.

Our results suggest that generative task-based identity representation holds transformative potential for diverse facial generation applications. We anticipate that this approach will inspire further innovation, broadening the capabilities and scope of generative identity modeling across a wider range of applications. Improvements in dataset scale and consistency, as well as the number and type of the decoders would further enhance robustness. Additionally, Omni-ID does not represent attributes that are not intrinsic to the face, such as hair, which can result in these features being “hallucinated” in downstream tasks. Extending Omni-ID to include a more comprehensive set of attributes remains an open direction for future research.

**Acknowledgement.** The authors would like to acknowledge other members of the Snap Creative Vision team for valuable feedback and insightful discussions throughout this project.

## References

- [1] Rameen Abdal, Yipeng Qin, and Peter Wonka. Image2stylegan: How to embed images into the stylegan latent space? In *Proceedings of the IEEE/CVF International Conference on Computer Vision*, pages 4432–4441, 2019. 2
- [2] Rameen Abdal, Peihao Zhu, Niloy J Mitra, and Peter Wonka. Styleflow: Attribute-conditioned exploration of stylegan-generated images using conditional continuous normalizing flows. In *ACM Transactions on Graphics (TOG)*, pages 1–21. ACM, 2020. 2
- [3] Black Forest Labs. Flux. <https://github.com/black-forest-labs/flux>, 2024. 2, 3, 6
- [4] Volker Blanz and Thomas Vetter. A morphable model for the synthesis of 3d faces. In *ACM Transactions on Graphics (SIGGRAPH)*, pages 187–194. ACM, 1999. 2
- [5] Chen Cao, Yanlin Weng, Shun Zhou, Yiyong Tong, and Kun Zhou. Facewarehouse: A 3d facial expression database for visual computing. *IEEE Transactions on Visualization and Computer Graphics*, 20(3):413–425, 2014. 2
- [6] Chaofeng Chen, Jiadi Mo, Jingwen Hou, Haoning Wu, Liang Liao, Wenxiu Sun, Qiong Yan, and Weisi Lin. Topiq: A top-down approach from semantics to distortions for image quality assessment. *IEEE Transactions on Image Processing*, 33:2404–2418, 2024. 6
- [7] Jiankang Deng, Jia Guo, Jing Yang, Niannan Xue, Irene Kotisa, and Stefanos Zafeiriou. ArcFace: Additive angular margin loss for deep face recognition. *IEEE Transactions on Pattern Analysis and Machine Intelligence*, 44(10):5962–5979, 2022. 1, 2, 6
- [8] Prafulla Dhariwal and Alexander Nichol. Diffusion models beat gans on image synthesis. *NeurIPS*, 34:8780–8794, 2021. 2
- [9] Rinon Gal, Yuval Alaluf, Yuval Atzmon, Or Patashnik, Amit H Bermano, Gal Chechik, and Daniel Cohen-Or. An image is worth one word: Personalizing text-to-image generation using textual inversion. *arXiv preprint arXiv:2208.01618*, 2022. 4
- [10] Rinon Gal, Moab Arar, Yuval Atzmon, Amit H Bermano, Gal Chechik, and Daniel Cohen-Or. Encoder-based domain tuning for fast personalization of text-to-image models. *ACM Transactions on Graphics (TOG)*, 42(4):1–13, 2023. 4
- [11] Rinon Gal, Or Lichter, Elad Richardson, Or Patashnik, Amit H Bermano, Gal Chechik, and Daniel Cohen-Or. Lcm-lookahead for encoder-based text-to-image personalization. *arXiv preprint arXiv:2404.03620*, 2024. 4
- [12] Zinan Guo, Yanze Wu, Zhuowei Chen, Lang Chen, and Qian He. Pulid: Pure and lightning ID customization via contrastive alignment. *CoRR*, abs/2404.16022, 2024. 4
- [13] Erik Härkönen, Aaron Hertzmann, Jaakko Lehtinen, and Sylvain Paris. Ganspace: Discovering interpretable gan controls. In *Advances in Neural Information Processing Systems*, pages 9841–9850, 2020. 2
- [14] Jonathan Ho. Classifier-free diffusion guidance. *ArXiv*, abs/2207.12598, 2022. 2
- [15] Jonathan Ho, Ajay Jain, and Pieter Abbeel. Denoising diffusion probabilistic models. *NeurIPS*, 33:6840–6851, 2020. 2
- [16] Edward J Hu, Yelong Shen, Phillip Wallis, Zeyuan Allen-Zhu, Yuanzhi Li, Shean Wang, Lu Wang, and Weizhu Chen. LoRA: Low-rank adaptation of large language models. In *ICLR*, 2022. 3, 4
- [17] Tero Karras, Samuli Laine, and Timo Aila. A style-based generator architecture for generative adversarial networks. In *CVPR*, pages 4401–4410, 2019. 2
- [18] Tianye Li, Timo Bolkart, Michael J. Black, Hao Li, and Javier Romero. Learning a model of facial shape and expression from 4D scans. *ACM Transactions on Graphics, (Proc. SIGGRAPH Asia)*, 36(6):194:1–194:17, 2017. 2
- [19] Zhen Li, Mingdeng Cao, Xintao Wang, Zhongang Qi, Ming-Ming Cheng, and Ying Shan. Photomaker: Customizing realistic human photos via stacked id embedding. *arXiv preprint arXiv:2312.04461*, 2023. 4, 8
- [20] Foivos Paraperas Papantoniou, Alexandros Lattas, Stylianos Moschoglou, Jiankang Deng, Bernhard Kainz, and Stefanos Zafeiriou. Arc2face: A foundation model of human faces. *CoRR*, abs/2403.11641, 2024. 6, 9
- [21] Alec Radford, Jong Wook Kim, Chris Hallacy, Aditya Ramesh, Gabriel Goh, Sandhini Agarwal, Girish Sastry, Amanda Askell, Pamela Mishkin, Jack Clark, et al. Learning transferable visual models from natural language supervision. In *International conference on machine learning*, pages 8748–8763. PMLR, 2021. 1, 2, 6
- [22] Elad Richardson, Yuval Alaluf, Or Patashnik, Yotam Nitzan, Yaniv Azar, Stav Shapiro, and Daniel Cohen-Or. Encoding in style: a stylegan encoder for image-to-image translation. In *Proceedings of the IEEE/CVF conference on computer vision and pattern recognition*, pages 2287–2296, 2021. 2
- [23] Robin Rombach, A. Blattmann, Dominik Lorenz, Patrick Esser, and Björn Ommer. High-resolution image synthesis with latent diffusion models. *2022 IEEE/CVF Conference on Computer Vision and Pattern Recognition (CVPR)*, pages 10674–10685, 2021. 2
- [24] Robin Rombach, Andreas Blattmann, Dominik Lorenz, Patrick Esser, and Björn Ommer. High-resolution image synthesis with latent diffusion models. In *CVPR*, pages 10684–10695, 2022. 2
- [25] Nataniel Ruiz, Eunji Chong, and James M. Rehg. Fine-grained head pose estimation without keypoints. In *The IEEE Conference on Computer Vision and Pattern Recognition (CVPR) Workshops*, 2018. 6
- [26] Nataniel Ruiz, Yuanzhen Li, Varun Jampani, Yael Pritch, Michael Rubinstein, and Kfir Aberman. Dreambooth: Fine tuning text-to-image diffusion models for subject-driven generation. In *CVPR*, pages 22500–22510, 2023. 4
- [27] Nataniel Ruiz, Yuanzhen Li, Varun Jampani, Wei Wei, Tingbo Hou, Yael Pritch, Neal Wadhwa, Michael Rubinstein, and Kfir Aberman. Hyperdreambooth: Hypernetworks for fast personalization of text-to-image models. *arXiv preprint arXiv:2307.06949*, 2023. 4

- [28] Jing Shi, Wei Xiong, Zhe Lin, and Hyun Joon Jung. Instant-booth: Personalized text-to-image generation without test-time finetuning. *arXiv preprint arXiv:2304.03411*, 2023. 4
- [29] Jiaming Song, Chenlin Meng, and Stefano Ermon. Denoising diffusion implicit models. *ArXiv*, abs/2010.02502, 2020. 2
- [30] Omer Tov, Yuval Alaluf, Yotam Nitzan, Or Patashnik, and Daniel Cohen-Or. Designing an encoder for stylegan image manipulation. *ACM Transactions on Graphics (TOG)*, 40(4): 1–14, 2021. 2
- [31] Andrey Voynov, Qinghao Chu, Daniel Cohen-Or, and Kfir Aberman.  $p+$ : Extended textual conditioning in text-to-image generation. *arXiv preprint arXiv:2303.09522*, 2023. 4
- [32] Hao Wang, Yitong Wang, Zheng Zhou, Xing Ji, Dihong Gong, Jingchao Zhou, Zhifeng Li, and Wei Liu. Cos-face: Large margin cosine loss for deep face recognition. In *CVPR*, pages 5265–5274. Computer Vision Foundation / IEEE Computer Society, 2018. 1, 2
- [33] Kuan-Chieh Wang, Daniil Ostashev, Yuwei Fang, Sergey Tulyakov, and Kfir Aberman. Moa: Mixture-of-attention for subject-context disentanglement in personalized image generation. *arXiv preprint arXiv:2404.11565*, 2024. 4
- [34] Qixun Wang, Xu Bai, Haofan Wang, Zekui Qin, and Anthony Chen. Instantid: Zero-shot identity-preserving generation in seconds. *arXiv preprint arXiv:2401.07519*, 2024. 4, 8
- [35] Ting-Chun Wang, Arun Mallya, and Ming-Yu Liu. One-shot free-view neural talking-head synthesis for video conferencing. In *Proceedings of the IEEE/CVF Conference on Computer Vision and Pattern Recognition (CVPR)*, 2021. 6
- [36] Liangbin Xie, Xintao Wang, Honglun Zhang, Chao Dong, and Ying Shan. VFHQ: A high-quality dataset and benchmark for video face super-resolution. In *CVPR Workshops*, pages 656–665. IEEE, 2022. 6
- [37] Hu Ye, Jun Zhang, Sibio Liu, Xiao Han, and Wei Yang. Ip-adapter: Text compatible image prompt adapter for text-to-image diffusion models. *arXiv preprint arxiv:2308.06721*, 2023. 2, 3, 4, 6
- [38] Jianhui Yu, Hao Zhu, Liming Jiang, Chen Change Loy, Weidong Cai, and Wayne Wu. Celebv-text: A large-scale facial text-video dataset. In *Proceedings of the IEEE/CVF Conference on Computer Vision and Pattern Recognition (CVPR)*, pages 14805–14814. IEEE, 2023. 6
- [39] Lvmin Zhang, Anyi Rao, and Maneesh Agrawala. Adding conditional control to text-to-image diffusion models, 2023. 4, 7
- [40] Yinglin Zheng, Hao Yang, Ting Zhang, Jianmin Bao, Dongdong Chen, Yangyu Huang, Lu Yuan, Dong Chen, Ming Zeng, and Fang Wen. General facial representation learning in a visual-linguistic manner. In *Proceedings of the IEEE/CVF Conference on Computer Vision and Pattern Recognition (CVPR)*, pages 18676–18688. IEEE, 2022. 1, 2
- [41] Hao Zhu, Wayne Wu, Wentao Zhu, Liming Jiang, Siwei Tang, Li Zhang, Ziwei Liu, and Chen Change Loy. Celebv-hq: A large-scale video facial attributes dataset. In *Proceedings of the European Conference on Computer Vision (ECCV)*, pages 650–667. Springer, 2022. 6
- [42] Zheng Zhu, Guan Huang, Jiankang Deng, Yun Ye, Junjie Huang, Xinze Chen, Jiagang Zhu, Tian Yang, Jiwen Lu, Dalong Du, et al. Webface260m: A benchmark unveiling the power of million-scale deep face recognition. In *Proceedings of the IEEE/CVF Conference on Computer Vision and Pattern Recognition*, pages 10492–10502, 2021. 6, 8